

# MOD 201 - Lab 2

Sasha Lanine

2024-03-19

## 1 Introduction

Neurons are able to propagate signals rapidly over long distances. They do this by generating electrical pulses, which we call an action potential or spike. Through these pulses, neurons are able to transmit information across the nervous system. In this report, we use computational experiments to investigate two key aspects of studying neural signaling. The first concerns *neural coding*. That is, how neurons encode information about stimuli through series of action potentials. The second aspect concerns the *generation of action potentials in a single neurons*. In particular, we will run simulations of several mathematical models of action potential generation.

## 2 Neural Coding: Spike Train Statistics

In this section, we will explore how to compute and analyze statistics about sequences of neuron spikes, which we call a *spike train*. By so doing, we will explore how we can use these techniques to better understand how neurons encode information about stimuli.

### 2.1 Modelling One Spike Train (1.1)

To begin, we need spike train data to analyze. Let us suppose that we wish to model a neuron that fires at rate  $r = 250 \text{ Hz}$  over a duration of  $T = 1 \text{ s}$ . To do this, we begin by partitioning the time interval into bins of equal-length, say  $\Delta t = 1 \text{ ms}$ . In each bin, we say that the neuron will fire with probability  $p = r\Delta t$  (assuming  $\Delta t$  is sufficiently small). For example, with the above parameters, we set  $p = \frac{1}{4}$ . To graphically depict the spike train, we use a raster plot, as shown in Figure 1. The  $x$ -axis corresponds to time. Vertical bars are present if the neuron fired at the corresponding time step.

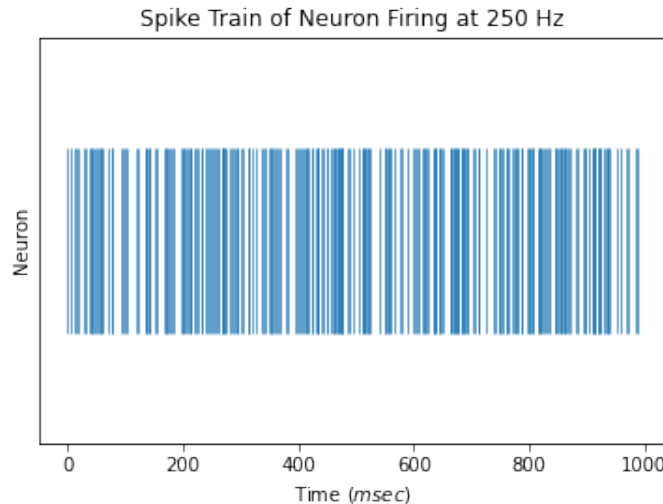
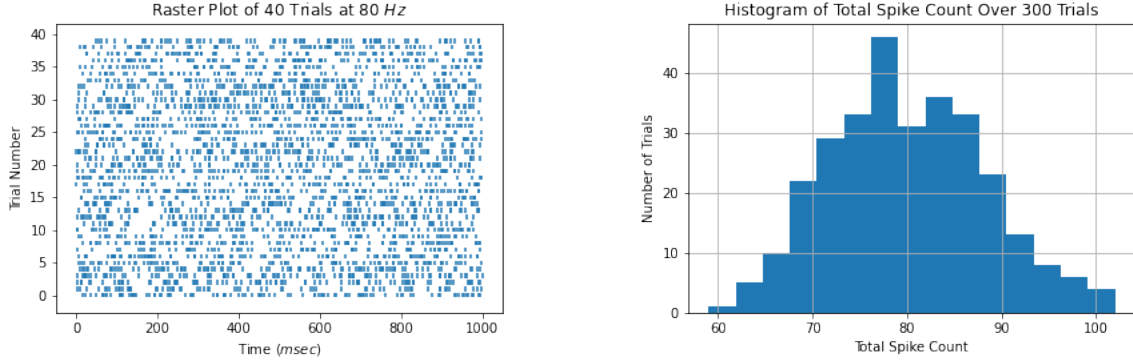


Figure 1: Spike train of one neuron that fires at an average rate of  $r = 250 \text{ Hz}$ .

### 2.2 Modelling Many Spike Trains (1.2, 1.4)

We can repeat this process to simulate one neuron firing at fixed rate over many trials. We ran  $N = 300$  such simulations with parameters  $r = 80 \text{ Hz}$ ,  $T = 1 \text{ s}$ , and  $\Delta t = 1 \text{ ms}$ . The results of the first 40 trials are depicted graphically in a raster plot in Figure 2a.



(a) Raster plot of the spike train of a neuron firing at an average of  $80 \text{ Hz}$  over 40 trials.

(b) Histogram of total spike counts for all  $N = 300$  trials with 15 bins.

Figure 2: Results of  $N = 300$  trials of a neuron firing at  $80 \text{ Hz}$ .

We also plot a histogram of total spike counts over all  $N = 300$  trials in Figure 2b. We find the data have a mean  $\mu = 80.2$  total spikes and standard deviation  $\sigma = 8.2$ , which is consistent with a firing rate of  $r = 80 \text{ Hz}$ .

Observe that the histogram in Figure 2b suggests that the total spike count statistic follows a roughly normal distribution. Indeed, this is what we should expect to happen. To see this, consider that whether a neuron fires in any given time-bin can be modelled as a Bernoulli Trial. That is, if we let  $X_i$  be a random variable describing the possible outcomes at  $i^{\text{th}}$  time step, then

$$\forall i, X_i = \begin{cases} 1, & \text{with probability } p \\ 0, & \text{with probability } 1 - p \end{cases}. \quad (1)$$

We then have that a random variable describing the total spike count is given by

$$Y = \sum_{i=1}^{T/\Delta t} X_i \quad (2)$$

That is,  $Y$  is the sum of  $T/\Delta t$  identical and (by assumption) independent random variables. It then follows by the *central limit theorem* that  $Y$  should approach a normal distribution as the number of trials approaches infinity. Thus we should not be surprised that the total spike count statistic approximates a normal distribution. Indeed, if we run this experiment again with a larger number of trials, it becomes more apparent that spike counts follow a normal distribution. Figure 3 shows the same experiment repeated for  $N = 10^4$  trials.

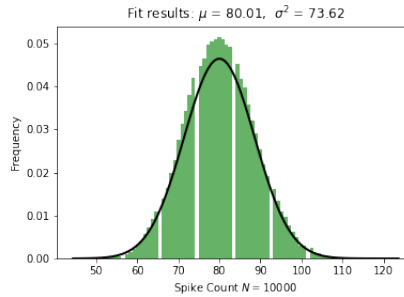


Figure 3: Total spike count histogram for  $N = 10^4$  trials with 80 bins.

### 2.3 The Inter-Spike Interval (1.3)

We now consider another useful spike-train statistic: the *inter-spike interval*. The inter-spike interval is defined as the time between two successive spikes in a spike-train. A histogram of the observed inter-spike intervals for the  $N = 300$  is shown in Figure 4 below.

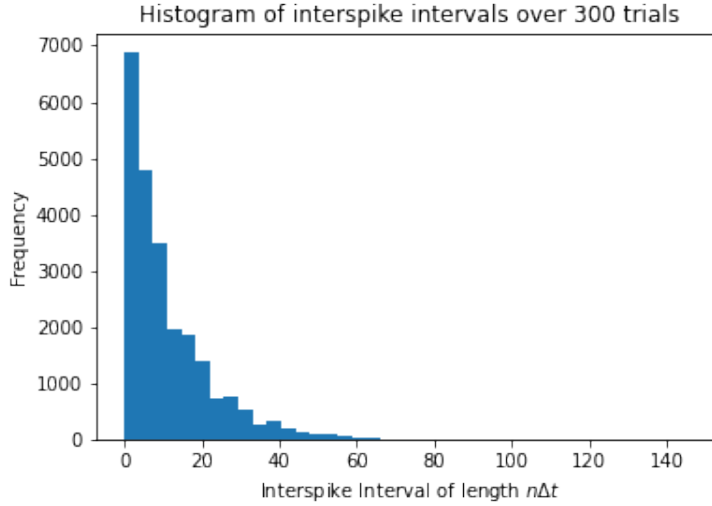


Figure 4: Histogram of interspike interval over 300 trials with 40 bins.

As  $\Delta t \rightarrow 0$ , we expect this probability distribution over inter-spike intervals to approach an exponential distribution with mean  $1/r$ , where  $r$  is the firing rate of the recorded neuron [1]. This explains the shape of the curve that we observe.

We also may calculate the *coefficient of variation*  $C_V$  of the observed data. This measures the variability of the time intervals between successive action potentials. It is of particular interest since we should expect  $C_V = 1$  if the spike trains are generated by a Poisson Process (which we expect in the  $\Delta t \rightarrow 0$  limit, see [1]). If  $C_V > 1$ , then this indicates that the spike train is less regular than a Poisson process (and more regular if  $C_V < 1$ ). For our data, we find that

$$C_V = \frac{\sigma_I}{\mu_I} \tag{3}$$

$$\approx \frac{11.8729}{11.3364} \tag{4}$$

$$\approx 1.05. \tag{5}$$

This indicates that our data is slightly less regular than a Poisson process.

### 2.4 Analyzing Real Spike-Train Data

We now begin to analyze real spike trains. The data was gathered from recordings of a single neuron in the primary somatosensory cortex of a monkey. The subject was presented with a vibratory stimulus on their fingertip at eight different frequencies. For each frequency, recordings for ten or twenty trials were taken.

#### 2.4.1 The First Stimulus (2.1-3)

We begin by considering the first stimulus of  $8.4 \text{ Hz}$ . A raster plot for the ten recorded trials at this frequency is shown in Figure 5

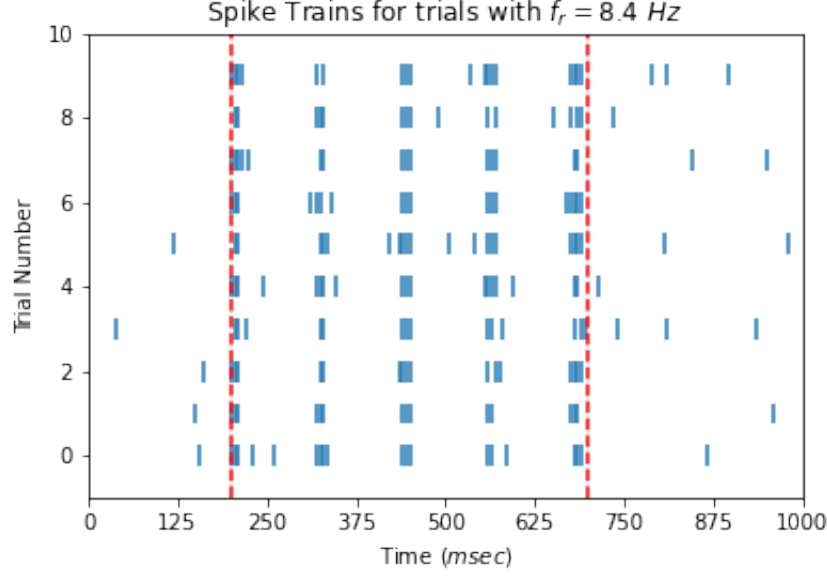


Figure 5: Raster plot for trials with stimulus of 8.4 Hz. The red bars denote the onset and end of the stimulus presentation (between 200msec and 700msec).

We observe that, on average, the neuron appears to begins to fire at a regular frequency during the stimulation period. We also find that, for the stimulation period, the trains have an average spike count of  $\mu = 16.5$  spikes with a variance of  $\sigma^2 = 3.25$ . We can use this to calculate the mean firing rate, which is given by

$$\bar{r} = \frac{\mu}{T} \quad (6)$$

$$= \frac{16.5 \text{ [spikes]}}{0.5 \text{ [s]}} \quad (7)$$

$$= 33 \text{ [spikes/s]}. \quad (8)$$

Another useful statistic to consider is the *spike density*, which is defined as the number of spikes occurring in each time window of length  $\Delta_t$ . That is, it is given by

$$\rho(t) = \frac{n_K(t; t + \Delta t)}{K}, \quad (9)$$

where  $K$  denotes the number of trials, and  $n_K(t; t + \Delta t)$  denotes the number of spikes occurring in the window  $(t, t + \Delta t)$  across all trials.

Using  $\Delta t = 5 \text{ [msec]}$ , the spike density for the first stimulus are shown below in Figure 6.

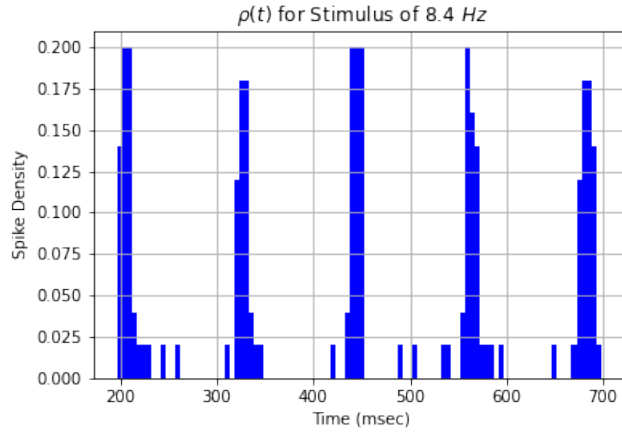


Figure 6: Spike density averaged over 10 trials for stimulus of 8.4  $Hz$ .

#### 2.4.2 Analyzing Data for all Stimuli

We now consider the spike trains for all trials and stimuli simultaneously. The collective spike trains are put in a raster plot show in Figure 7.

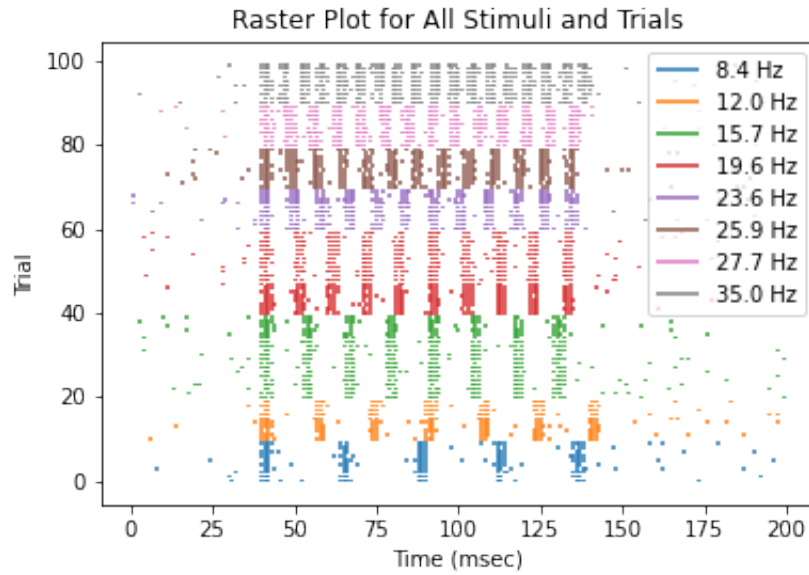


Figure 7: Raster plots for all trials. Trials are grouped by the stimulus frequency.

Again, we can also compute the spike densities across trials for each stimulus. The results are shown in Figure 8.

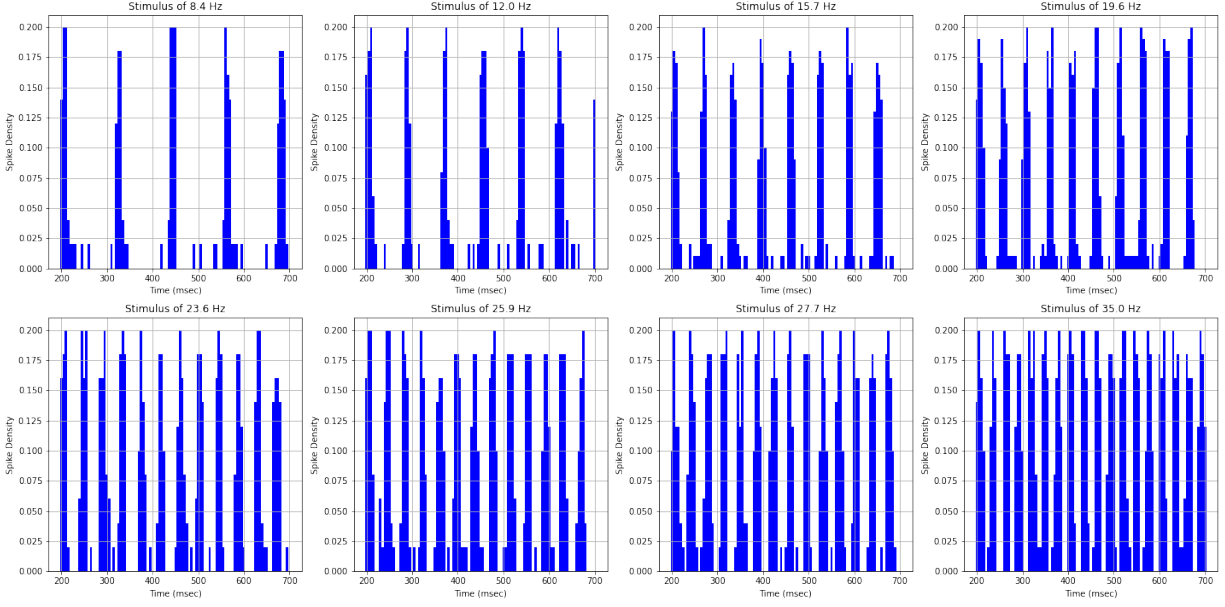


Figure 8: Spike density plot for each of the eight stimuli frequencies.

We see that an increase stimulus leads to an apparent increase in the firing rate of the recorded neuron. To investigate this relation further, we compute the mean and variance of the spike counts for each stimulus, as well as the mean firing rate. The results are summarized in table

	8.4 Hz	12 Hz	15.7 Hz	19.6 Hz	23.6 Hz	25.9 Hz	27.7 Hz	36 Hz
$\mu_{count}$	16.5	19.9	23.6	29.9	35.6	39.5	41.8	52.9
$\sigma^2_{count}$	3.25	2.09	3.84	2.49	6.24	8.65	3.56	11.09
$\bar{r}$	33	39.8	47.2	59.8	71.2	79	83.6	105.8

Table 1: Table summarizing mean and variance of spike counts, as well as mean firing rates, for each stimulus frequency.

To further investigate the relationship between the stimulus frequency and the mean firing rate, we plot them against each other in Figure 9.

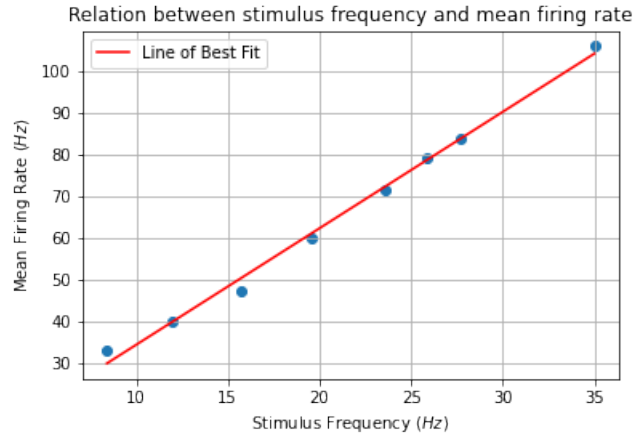


Figure 9: A linear relation is when plotting mean firing rate against stimulus frequency.

We observe that it appears that the mean firing rate scales linearly with the stimulus frequency. Indeed a line of best fit was found to be  $y \approx 2.8x + 6.3$ , and had a standard error of only  $SE \approx 2$ , which indicates that the data is reasonably well-fitted to the regression line. This suggests that the recorded neuron is encoding the strength of the stimulus.

### 3 Single Neuron Modelling

We now switch our attention to models of action potential generation in a single neuron. There are two types of models we will consider, both derived from modelling a neuron as an electrical circuit. The first models are variants of the *integrate and fire model*. The second model we will consider is the more bio-physically *Hodgkin-Huxley model*.

#### 3.1 Integrate and Fire

The basic governing equation of integrate and fire models is the following:

$$C \frac{dV(t)}{dt} = g_L(E_L - V(t)) + I, \quad (10)$$

where  $C$  is the neuron membrane capacitance,  $g_L$  is the conductance,  $V(t)$  is the membrane potential,  $I$  is the input current, and  $E_L$  is the reversal potential.

In what follows, we will set the parameters as follows:  $C = 1nF$ ,  $g_L = 0.1\mu S$ , and  $E_L = -70mV$ . In Figure 10 we plot numerically integrated solutions to Equation 10 for varying time-constant input currents (setting  $V(0) = E_L$ ).

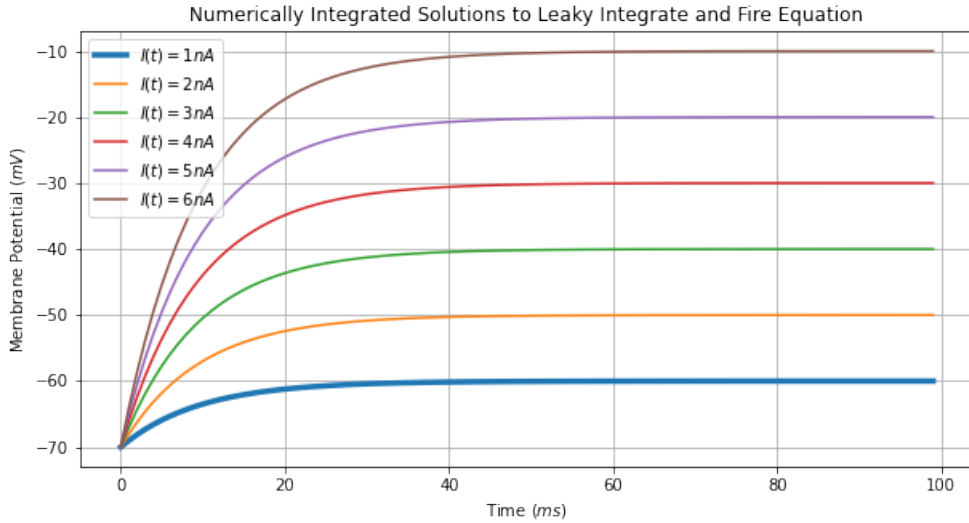


Figure 10: Numerically integrated solutions to integrate and fire equation.

We see that across cases the membrane potential appears to increase and asymptotically converge to a fixed value. Furthermore, the limiting value appears to scale linearly with  $I$ . To better understand this, let us compare our findings to the analytic solution to Equation 10.

We begin by re-writing Equation 10 as

$$\frac{dV(t)}{dt} = -\frac{g_L}{C}V(t) + \frac{1}{C}(I + g_LE_L). \quad (11)$$

Making the substitutions  $a = -\frac{g_L}{C}$  and  $b = \frac{1}{C}(I + g_LE_L)$ , we see that the problem reduces to solving the equation

$$\frac{dV(t)}{dt} = aV(t) + b. \quad (12)$$

The solution to this equation is given by

$$V(t) = e^{at}V(0) + e^{at} \int_0^t e^{-as}b ds \quad (\text{See, for example, [2]}) \quad (13)$$

$$= e^{at}V(0) + \frac{b}{a}(e^{at} - 1) \quad (\text{Assuming constant } I). \quad (14)$$

$$(15)$$

Back-substituting  $a$  and  $b$ , and setting  $V(0) = E_L$ , we find our solution is given by

$$V(t) = e^{-\frac{g_L}{C}t}E_L - \frac{I + g_LE_L}{g_L}(e^{-\frac{g_L}{C}t} - 1). \quad (16)$$

We then find that

$$\lim_{t \rightarrow \infty} V(t) = \frac{I + g_LE_L}{g_L} \quad (17)$$

This confirms one of our observations:  $V(t)$  will converge to a potential that scales linearly with  $I$ .

### 3.1.1 Adding a Spiking Mechanism

Observe that the current iteration of the integrate and fire model has no means of generating action potentials. It will only monotonically converge to a membrane potential in time. To fix this, we implement a kind of ‘spike-pasting’ method. When the membrane potential passes a threshold  $V_{th} = -63mV$ , we will force the numerical integrator to set the voltage at the next time step to  $V_{max} = 30mV$ . At the time step after that, we will reset the voltage to  $V = E_L$ , mimicking an action potential. Figure 11 depicts the result of rerunning simulation from the previous section with  $I = 1nA$ .

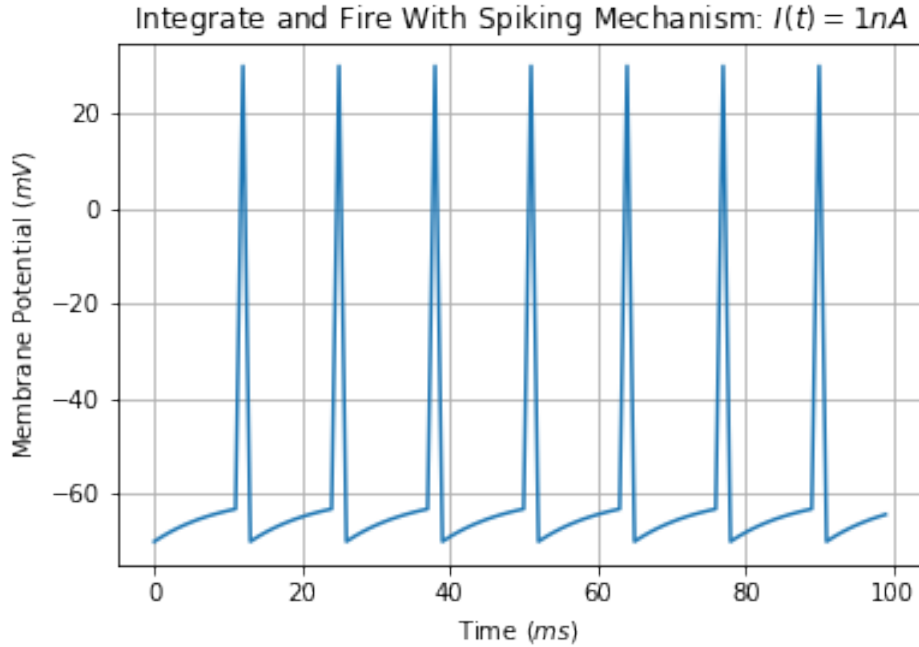


Figure 11: Integrate and fire with spiking mechanism simulation.



We see now that the neuron “fires” at regular intervals.

Note that the current will not fire for all values of  $I$ . Indeed, our analytic work shows that we would need that

$$\frac{I + g_L E_L}{g_L} > V_{th} \Rightarrow I > 0.7nA \quad (18)$$

for this to occur.

We can test this prediction by using bisection method on values of  $I$ , searching for the first value at which the neuron produces an action potential. With an error tolerance  $10^{-10}$ , we found a threshold value of  $I_{th} \approx 0.70002nA$ , consistent with the analytic prediction.

To conclude this section, we plot the tuning curve of the neuron in Figure 12. That is, the number of spikes that occur in the given time-window as a function of the input current.

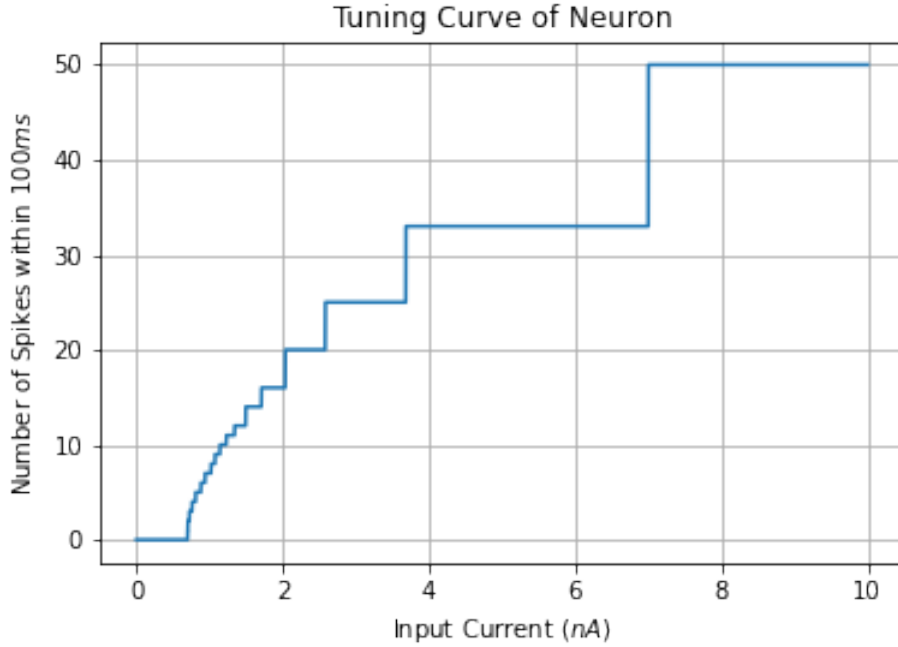


Figure 12: Tuning curve of neuron as function of input current.

### 3.1.2 Adding Noise

We can now make the spiking dynamics more realistic by adding a noise term  $\sigma\eta(t)$ , where  $\eta(t)$  is a random variable from the standard normal distribution, and  $\sigma$  is a factor that controls for the magnitude of the noisy perturbation. Thus our new equation becomes

$$C \frac{dV}{dt} = g_L(E_L - V) + I + \sigma\eta(t). \quad (19)$$

A glimpse of how this affects the spiking dynamics can be seen in Figure 13.

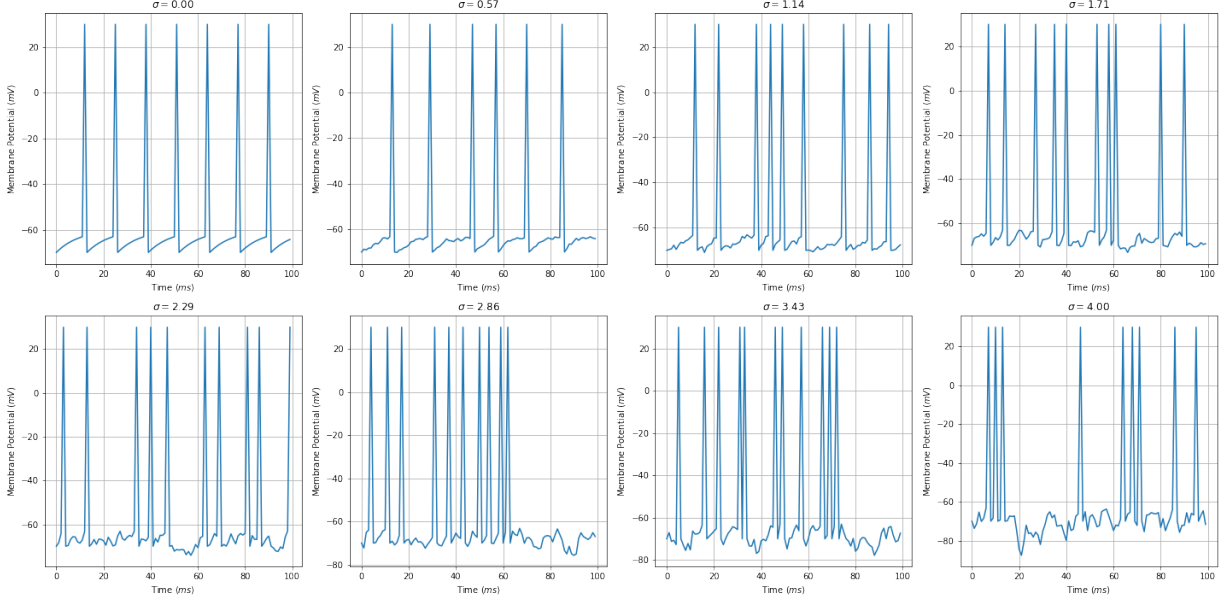


Figure 13: Numerically integrated solutions for noisy integrate and fire with  $I = 1nA$  and varying values of  $\sigma$ .

Further, Figure 14 depicts a raster plot for spike-trains generated with increasingly large values of  $\sigma$ .

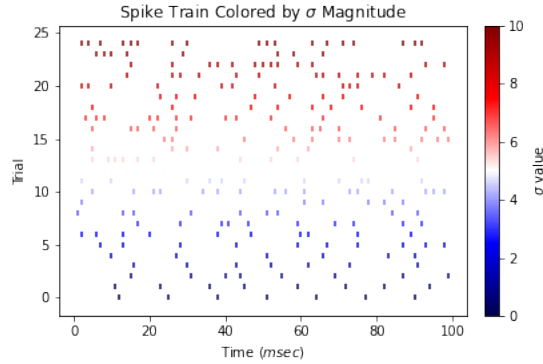


Figure 14: Raster plot of spike trains generated for different values of  $\sigma$ .

We see that increase in  $\sigma$  lead to increases in spike count for for small values of  $\sigma$ . It is unclear, however, if this trend continues or would persist in larger datasets. Further investigation is needed to understand the relationship between  $\sigma$  and spike count.

### 3.1.3 Time Dependent Input

We now consider the case where the input current is time-dependent. That is, the governing equation becomes

$$C \frac{dV}{dt} = g_L(E_L - V) + I(t) + \sigma \eta(t). \quad (20)$$

For example, we could have current that is constant for a given time window, but otherwise constant:

$$I(t) = \begin{cases} 1, & t_1 \leq t \leq t_2 \\ 0, & \text{else} \end{cases}. \quad (21)$$

The results of such dynamics are depicted in Figure 15 below. Note that we hold  $\sigma = 0.5$  to avoid large effects from the noise term.

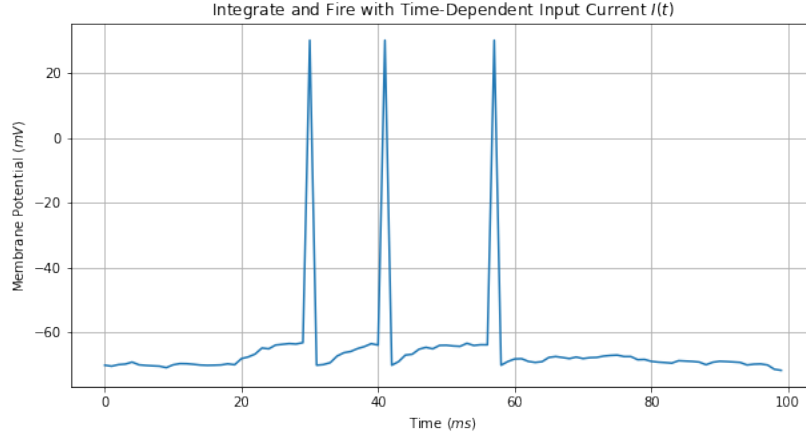


Figure 15: Numerically integrated solution to integrated solution to integrate and fire with  $I(t) = \mathbb{1}_{t \in [t_1, t_2]}$ .

We now consider the following question: what kind of current would  $I(t)$  need to be to generate spike trains like those of Section 2.

To begin to answer this question, recall that we assumed in Section 2 that the neuron fired with some probability  $p$  at each time step. The following function will then suffice to mimic these dynamics.

$$I(t, t + \Delta t) = \begin{cases} 50nA & \text{with probability } p \\ 0nA & \text{with probability } 1 - p \end{cases}. \quad (22)$$

That is, at each time steps,  $I(t)$  we deliver an impulse sufficiently strong to trigger an action potential with probability  $p$ <sup>1</sup>

Using this method, we simulate a neuron that fires at 250 Hz. We plot its spike train below in Figure 16.

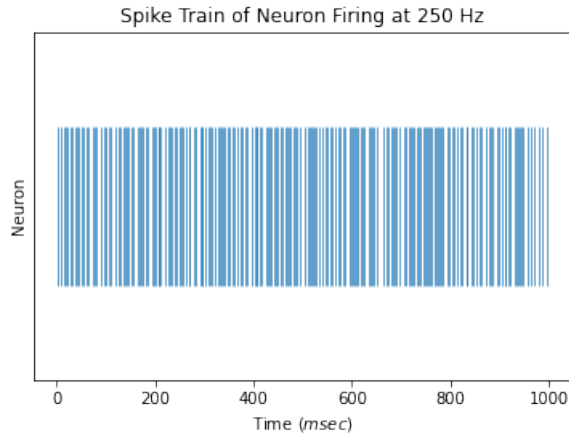


Figure 16: Spike train generate with Bernoulli-like input current.

<sup>1</sup>There is a small technicality here: in the time step immediately following an action potential, it is impossible for the neuron to fire again using the spiking mechanism. To remedy this, we double the probability  $p$  that we would otherwise use.

### 3.2 Hodgkin-Huxley Model

We now turn our attention to the Hodgkin-Huxley model: an extension of the integrate that incorporates how the dynamics at voltage-gated ion channels impact the spiking mechanism. This leads to a model with more bio-physically realistic dynamics. It is governed by the following equation:

$$C \frac{dV}{dt} = g_L(E_L - V) + \bar{g}_K(E_K - V) + \bar{g}_{Na} m^3 h (E_{Na} - V) + I \quad (23)$$

For what follows, we set the parameters as follows:  $C = 1 \mu F/cm^2$ ,  $g_K = 36 mS/cm^2$ ,  $E_K = -77 mV$ ,  $g_{Na} = 120 mS/cm^2$ ,  $E_{Na} = 50 mV$ ,  $g_L = 0.3 mS/cm^2$ , and  $E_L = -54.4 mV$ .

The terms  $n$ ,  $m$  and  $h$  are *gating variables*. They capture represent the probability of ion channel gates being open or closed, controlling the flow of specific ions across the neuron's membrane and thus influencing the neuron's electrical behavior. Their dynamics are governed by differential equations of the form

$$\frac{dx}{dt} = \alpha(V)(1 - x) - \beta(V)x, \quad (24)$$

where  $\alpha$  and  $\beta$  are the voltage-dependent open and closing rates, respectively.

We plot the results of numerically integrating  $V(t)$ ,  $n(t)$ ,  $m(t)$ , and  $h(t)$  for  $I = 8 nA/cm^2$  in Figure 17.

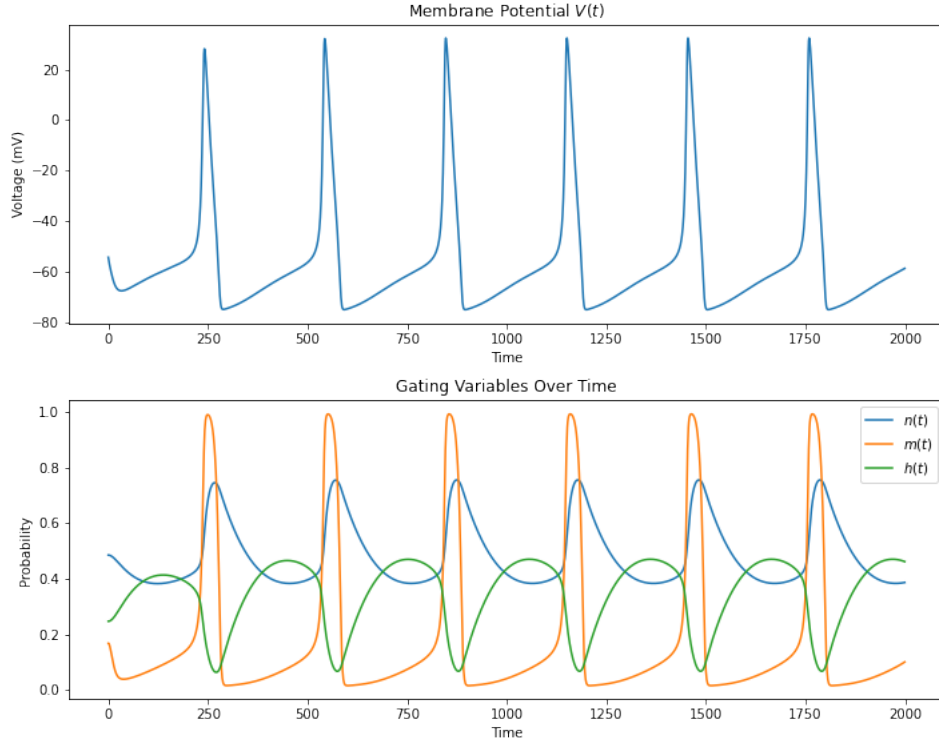


Figure 17: Result of numerically integrating Hodgkin-Huxley equations for  $I = 1 nA/cm^2$ .

We would like to investigate when the neuron will start firing as we increase the input current from  $I = 0$  to  $I = 10$ . To do this, we again use a bisection method on the interval  $[0, 10]$ . The results of setting the error tolerance to  $10^{-10}$  yields a threshold value of  $I_{th} \approx 7.946$ . Further, by investigating spike-counts (measured from onset of spiking), we find that the the lowest firing rate is approximately  $6 Hz$ . At the spiking threshold, however, we see that it takes awhile for the spike to occur, after which point it begins firing at  $6 Hz$  for all future time.

## 4 Conclusion

In the initial part of our study, we discovered that analyzing various statics of spike trains serves as a robust approach to understand how neurons encode information about stimuli. This was exemplified by identifying an almost linear correlation between stimulus intensity and the average firing rate across trials in the monkey experiment.

Subsequently, our exploration into the utility of electrical circuit-inspired models for simulating neuron spiking behavior in a singular neuron revealed significant insights. Progressing through progressively sophisticated iterations of the integrate-and-fire model, culminating in the Hodgkin-Huxley model, enabled us to construct more biophysically accurate models of action potential generation.

## References

- [1] Peter Dayan and L. F. Abbott. *Theoretical Neuroscience: Computational and Mathematical Modeling of Neural Systems*. The MIT Press, 2001.
- [2] G. Strang. *Differential Equations and Linear Algebra*. Wellesley, 2015.